Support Recovery for Multiband Spectrum Sensing Based on Modulated Wideband Converter with SwSOMP Algorithm

Zhuhua Hu[1,2], Yong Bai[1,2(✉)], Yaochi Zhao[2], and Yiran Zhang[2]

[1] State Key Laboratory of Marine Resource Utilization in South China Sea, Hainan University, No. 58, Renmin Avenue, Haikou 570228, Hainan Province, People's Republic of China
{eagler_hu, bai}@hainu.edu.cn
[2] College of Information Science and Technology, Hainan University, No. 58, Renmin Avenue, Haikou 570228, Hainan Province, People's Republic of China

Abstract. The Modulated Wideband Converter (MWC) can provide a sub-Nyquist sampling approach to sense sparse multiband analog signals and reconstruct the frequency support set. However, the existing SOMP reconstruction algorithms need a priori information of signal sparsity. This paper applies the SwOMP algorithm to the CTF (Continuous-To-Finite) block of MWC. The SwSOMP algorithm uses stage-wise weak selection in SOMP, and it can reduce computational cost and solve large scale problems. It does not need prior information of signal sparsity, and the frequency support can be reconstructed blindly. The simulation results demonstrate that, MWC system with SwSOMP algorithm, compared with the SOMP algorithm, can use less number of channels, achieve higher percentage of correct support recovery blindly, and reduce the sampling rate of the system.

Keywords: Spectrum sensing · MWC · sub-Nyquist sampling
Compressed sensing · Stage-wise weak Simultaneous OMP(SwSOMP)

1 Introduction

Spectrum sensing is often necessary in communication applications, such as Cognitive Radio (CR) [1]. Its aim is to solve the spectrum crowdedness. CR should be able to reliably monitor the spectrum and detect the primary users (PUs) activity. Then, secondary users (SUs) would opportunistically access frequency bands left vacant by PUs. Therefore, support recovery of signals is pivotal to exploit the vacant bands in wideband spectrum. Generally, the sparse multi-band analog signal is transmitted in CR network. Multiband RF signals occupy a fairly wideband range, while the frequency band of each RF signal is narrow and distributed within the given bandwidth without intersecting.

At the receiver, if the Nyquist sampling theorem is used to reconstruct the high frequency multiband analog signal, it brings the sampling system a burden of ultra-high sampling rate and massive sampling data [2]. Therefore, in order to achieve sub-Nyquist sampling rate, the compressed sensing theory [3] must be extended to the

K. Long et al. (Eds.): 5GWN 2017, LNICST 211, pp. 146–159, 2018.
https://doi.org/10.1007/978-3-319-72823-0_15

analog domain. First came the method based on AIC (Analog-to-Information Conversion) [4, 5]; However, the application scenarios of AIC is limited, and sampling efficiency for the multiband signal is low. For this reason, a variety of novel sub-Nyquist sampling structures have emerged such as CRD (Constrained Random Demodulation) [6], random equivalent sampling [7] and MWC (Modulated Wideband Converter) [8]. The sub-Nyquist sampling method of MWC is proposed by Yonina Eldar and can be applied in the field of radar [9], broadband communication [10] and cognitive radio spectrum sensing [11, 12].

The accurate reconstruction of the signal support set is the core problem of MWC system. At present, MWC mainly uses CTF (Continuous-To-Finite) reconstruction block [13]. SOMP (Simultaneous Orthogonal Matching Pursuit) algorithm [14] can be used commonly as the reconstruction algorithm in CTF block. SOMP is simple and easy to realize, but its probability of correct reconstruction is not high enough [15]. Under the case of no noise, the required number of channels for accurate reconstruction is much higher than the theoretical lower bound. In practical applications, the channels must be implemented by the hardware, which will greatly increase the development cost of the system. In addition, the sparsity of signal has to be used as a priori information for the reconstruction. However, it is difficult to obtain in the CR environment. Therefore, it is important to investigate better reconstruction algorithms which do not depend on the signal sparsity, and can significantly improve the percentage of the support recovery and can reduce the number of required sampling channels.

To address the existing problems, this paper applies the SwSOMP (Stage-wise weak Simultaneous OMP) algorithm based on SwOMP [16] to the support recovery of MWC. The SwSOMP algorithm uses stagewise weak selection in SOMP, it further improves StOMP (Stage-wise OMP) [17] and optimizes the threshold settings for the selection of atoms, which can reduce the dependency for the observation matrix. It can reduce computational cost and solve large scale problems. It does not need prior information of signal sparsity, and the frequency support can be reconstructed blindly. This paper applies the SwSOMP algorithm to the CTF (Continuous-To-Finite) block of MWC. The simulation results demonstrate that, MWC system with SwSOMP algorithm can use less number of channels, achieve higher percentage of correct support recovery blindly, and further reduce the sampling rate of the system.

The remainder of this paper is organized as follows. In Sect. 2 we introduce the signal model and principles of MWC system. Section 3 describes the method of support recovery of MWC with SwSOMP algorithm. Section 4 gives the simulation results and discussion. Section 5 concludes this paper.

2 Signal Model and Principles of MWC System

2.1 Sparse Multiband Signal Model

Sparse multiband signal is often found in the CR environment [18]. Suppose that the received signal $x(t)$ is a sparse bandpass analog signal. Its spectrum is distributed in the frequency range $[-f_{nyq}/2, f_{nyq}/2]$, and f_{nyq} is the Nyquist sampling rate of the signal. Assume that the spectrum of $x(t)$ only contains N sub-bands whose bandwidth are

$B_i \leq B \ \ (N \geq i > 0)$ (without considering the symmetric band), and the sub-bands do not overlap. B is the maximum bandwidth of the sub-bands. The center carrier frequency of each sub-band is unknown. All unions of sub-bands and the maximum bandwidth B can be expressed as:

$$P_{2N} = \bigcup_{1}^{N} \{(a_i, b_i) \cup (-b_i, -a_i)\} \ \ B = \max_i (b_i - a_i) \tag{1}$$

The minimum needed sampling rate of the multi-band signal, the Landau rate [19], is defined as:

$$M(P_{2N}) = 2 \sum_{i=1}^{N} (b_i - a_i) \tag{2}$$

As is shown in Fig. 1, the entire frequency band is divided into L continuous narrow bands, and each band's bandwidth is not larger than B. Adding the symmetric parts, the spectrum of $x(t)$ in the entire frequency band has at most $2N$ parts with signal energy. The bands are designated as $[1, \ldots, L]$, then the set of the indices of sub-band $X_i(f)$ is called the support set of signal $x(t)$ which is defined as $\Lambda = \text{supp}(X(f))$. The frequency bands corresponding to the indices are called the support bands. Since $2N \ll L$, $x(t)$ can be viewed as a sparse multiband signal.

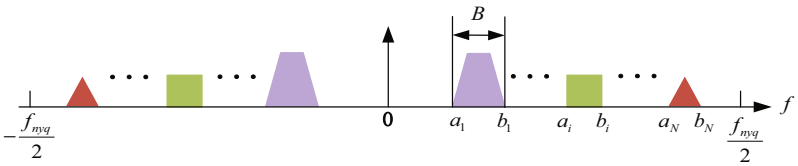

Fig. 1. Spectrum structure of sparse multiband signal

In summary, the support bands of $x(t)$ must meet the following two conditions: (1) it has to be distributed in a very wide frequency range; (2) the signals only exist in a few discrete frequency bands.

2.2 Sampling Scheme for MWC System

MWC contains a number of sampling channels, and each channel structure is the same, which is composed of the mixer, low-pass filter and ADC. The structure of the system is shown in Fig. 6(a). The received signal $x(t)$ is input into m parallel channels at the same time, each of which multiplies different patterns of periodic mixing signal $p_i(t)$ to realize the shifting from the frequency spectrum of $x(t)$ signal to baseband. The $p_i(t)$ of each channel is uncorrelated, and the cycle of $p_i(t)$ is $T_p = 1/f_p$. M is used to show the number of random alternating times of ± 1 in a cycle. Mf_p is defined as the alternating frequency of the mixing signal. The waveform of $p_i(t)$ is shown in Fig. 2. After

mixing, the signal passes through lowpass filter whose cut-off frequency is $1/2T_s$, as is shown in Fig. 3. It finally passes through ADC at sampling rate is $f_s = 1/T_s$ and acquires M groups of low-speed digital sampling sequence $y_i[n]$.

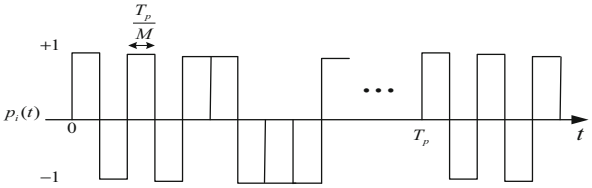

Fig. 2. Periodic mixing signal of the ith channel

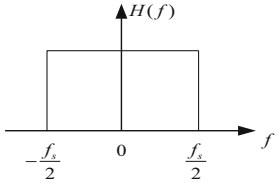

Fig. 3. Ideal low-pass filter.

On the analysis of the ith channel, the Fourier series expansion of the random mixing function $p_i(t)$ is:

$$p_i(t) = \sum_{l=-\infty}^{\infty} c_{il} e^{j2\pi f_p l t} \tag{3}$$

The coefficient $c_{il} = d_l \sum_{k=0}^{L-1} \alpha_{ik} e^{-j\frac{2\pi}{L}lk}$, $\alpha_{ik} \in \{-1, +1\}$. When $l = 0$, $d_0 = 1/L$, and when $l \neq 0$, $d_l = (1 - e^{-j\frac{2\pi l}{L}})/j2\pi l$.

Then, after passing through the lowpass filter with frequency characteristic $H(f) = \begin{cases} 1 & |f| \leq f_s/2 \\ 0 & |f| > f_s/2 \end{cases}$, the relationship between the DTFT (Discrete Time Fourier Transform) of $y_i[n]$ and $x(t)$'s Fourier transform $X(f)$ is obtained by sampling is as follows:

$$Y_i(e^{j2\pi f T_s}) = \sum_{l=-L_0}^{L_0} c_{il} X(f - l f_p) \tag{4}$$

In (4), $f \in [-f_s/2, f_s/2]$, and L_0 is the smallest integer that makes $L = 2L_0 + 1 \geq F = f_{nyq/f}$. The Eq. (4) shows that the spectrum of the output sequence $Y_i[n]$ is changed to the weighted sum of original signal spectrum $X(f)$ with a f_p step shifts, and the spectral segment with a width of f_s is intercepted by a low-pass filter. If taking $Y_i(e^{j2\pi f T_s})$ as the ith component of m dimensional column vectors, $X(f - l f_p)$ as the lth components of the $2l_0 + 1$ dimensional column vectors $z(f)$, (4) can be expressed as:

$$y(f) = \Phi z(f), \quad f \in [-f_s/2, f_s/2] \tag{5}$$

In (5), Φ is a $m \times L$ matrix. $\Phi_{il} = c_{i,-l} = c_{il}*, 1 \leq i \leq m$, and $m < L$. Applying IDTFT (Inverse Discrete Time Fourier Transform) transform on (5), we can get the corresponding relationship between the sequence $Z[n] = [z_1[n], z_2[n], \ldots, z_L[n]]^T$ and the sampling data $Y[n] = [y_1[n], y_2[n], \ldots, y_m[n]]^T$.

$$Y[n] = \Phi Z[n] \tag{6}$$

For any frequency $f \in [-f_s/2, f_s/2]$, (6) can be viewed as a typical compressed sensing problem, where an observed vector Y is known to recover an unknown sparse vector Z. Therefore, it is viable to recover the support bands of the signal by using the reconstruction algorithms of compressed sensing.

2.3 Reconstruction of Signal Support Set

Since $m < L$, (5) is an underdetermined equation. To get the unique solution to the equation, the sampling parameters of the MWC system must meet the following conditions [8]:

(1) $f_s \geq f_p \geq B, \frac{f_s}{f_p} < \frac{M_{\min}+1}{2}$;
(2) $m \geq 2K = 4N$, K is the sparsity of the sparse vector $z(f)$. N is the number of signal bands without considering the symmetric bands;
(3) The number of ± 1 symbols in a periodic sequence $p_i(t)$ must satisfy $M \geq M_{\min} = \left\lceil \frac{f_{nyq}}{f_p} \right\rceil$. If $f_s = f_p$, then $M_{\min} = L$;
(4) Any $4N$ column of the matrix Φ is linearly independent.

It has been pointed out in [3] that the sparse solution for (5) is a NP-hard problem. Nonetheless, such a problem can be transformed into a minimization of the l_1 norm problem provided that the number of sampling channels $m \geq cK \log(L/K)$. c is a constant, and K is the sparsity (i.e. the number of signal bands). It can be known that the value of m is much greater than $2K$.

The crucial problem of reconstruction is to reconstruct the sparse $Z[n]$ from the sampling sequences $Y[n]$. Since the signal frequency is continuous in $[-f_s/2, f_s/2]$, (5) is infinite dimensional, i.e., contains infinite number of SMV (Single Measurement Vector) problem. A CTF block is proposed for reconstruction in [13], as shown in the Fig. 4. It was proposed as a transformation framework from infinite dimension to finite dimension (Multiple Measurement Vectors, MMV) [15]. Support bands Λ of the signal can be estimated by CTF, through which the signal $x(t)$ can be further recovered. SOMP algorithm can be used to the reconstruction in MWC, which achieves reconstruction in [8]. The experimental results show that algorithm can achieve high percentage of correct reconstruction when $m \geq 2K \log(L/K)$, but there is still a large gap compared with the theoretical lower bound.

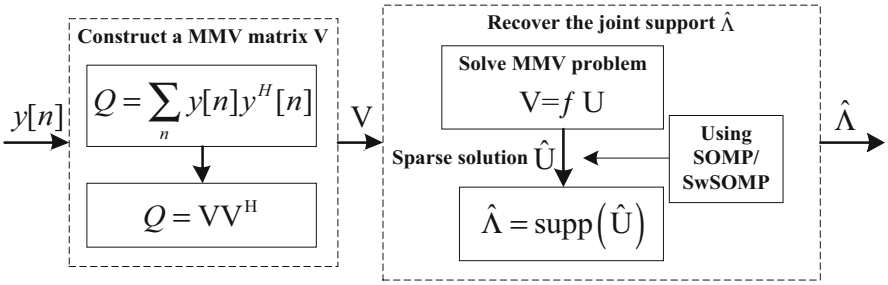

Fig. 4. Schematic diagram of the CTF block.

3 Support Recovery of MWC with SwSOMP Algorithm

As mentioned in the introduction, the SOMP reconstruction algorithm has many shortcomings. As a result, in terms of the success rate of recovery, the needed minimum number of channels, the reconstruction under low SNR and the maximum number of bands that can be reconstructed, the reconstruction algorithm of MWC still has a large space for improvement.

SwSOMP adopts the idea of stage-wise. First, atoms are selected according to the principles of correlation, using threshold to select atoms matched with residual. The difference with SOMP algorithm is that it does not always choose the most relevant matching atom in each iteration, but finds a number of atoms in each iteration according to atomic selection criteria. Then support set and support matrix are updated, least square method is used to obtain an approximate solution, and the residual is updated finally. At last, the support Λ is obtained after the end of the iterations. The procedure of SwSOMP algorithm is shown in the Fig. 5.

The threshold of the atomic selection of the algorithm is defined as:

$$th = \alpha \max_i |g_i| \tag{7}$$

where g represents the correlation matrix obtained after inner product operation with observation matrix Φ and the residual. (7) finds out the largest correlated data in the matrix and uses its index in the matrix to find the corresponding atom in the column of Φ. The chosen atom is most relevant with the residual. α is known as weakness parameter and $\alpha \in (0, 1]$. The reason of such a threshold selection is that the obtained largest value of the inner product operation sometimes may not be the most relevant one. According to (7), the updated expression of the corresponding support set in SwSOMP is:

$$\Lambda_k = \Lambda_{k-1} \cup \{i : |g_i| \geq th\} \tag{8}$$

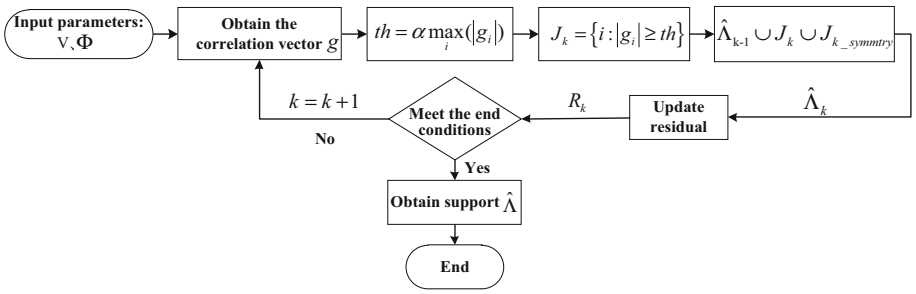

Fig. 5. Procedure of SwSOMP algorithm.

Although the StOMP algorithm does not rely on the signal sparsity, but there is a close relationship between the settings of selection threshold and observation matrix. Threshold obtained in [17] is only for random Gaussian matrix, thus limits the application of StOMP. On the other hand, the SwOMP algorithm has no strict requirement for the observation matrix, and does not need to know the signal sparsity, thus reduces the matching times, and improves the efficiency of the reconstruction. In the corresponding MMV problem of MWC, compared to the SMV problem handled in SwOMP, the one-dimensional sampling vector becomes two-dimensional sampling matrix Y. The MWC reconstruction process with SwSOMP algorithm is shown in Fig. 6.

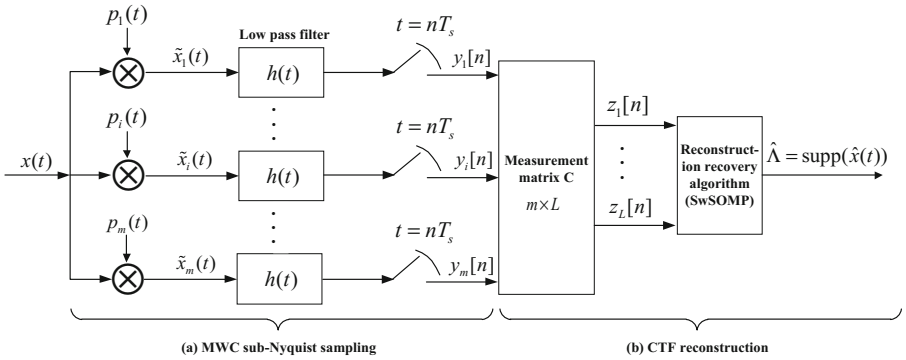

Fig. 6. MWC reconstruction process with SwSOMP.

The SwSOMP algorithm is a greedier approach for finding sparse solutions of underdetermined system. It selects several new elements in each iteration. The algorithm is described as Table 1. In Table 1, e_j is the unit column vector of the jth element that equals 1. The function of *diag* is to take the diagonal elements of the matrix. $\Lambda_{symmetry}$ is the symmetric support bands. $\Phi_{\hat{\Lambda}_k}$ is the sub-matrix of observation matrix, and $\Phi_{m\times L}$ corresponds to the support band $\hat{\Lambda}_k$.

Table 1. The reconstruction algorithm of support with SwSOMP

Input: observation matrix $\Phi_{m\times L}$;
mesurements $V_{m\times d}$;
iterations $Iters$;
the threshold of the residual ε_1;
the threshold of the ratio of residual to estimated solution ε_2.

Initialization: the initial support of the signal band $\hat{\Lambda}_0 = \varnothing$, initial residual $R_0 = V$.

For $k = 1$ **to** $Iters$

Identification: $g = \left\| \sum_{j=1}^{d} \left| \Phi^H (R_{k-1} e_j) \right| \right\|_2 ./ \sqrt{diag(\Phi^H \Phi)}$.

$$J_k = \left\{ i : g_i \geq \alpha \max_i (g_i) \right\}.$$

$$\Lambda_{symmetry} = L + 1 - J_k.$$

Augmentation: $\hat{\Lambda}_k = \hat{\Lambda}_{k-1} \bigcup J_k \bigcup \Lambda_{symmetry}$, then obtain $\Phi_{\hat{\Lambda}_k}$.

Estimation: $\hat{\Theta}_k = \Phi_{\hat{\Lambda}_k}{}^{+} V$, and $\Phi_{\hat{\Lambda}_k}{}^{+} = (\Phi_{\hat{\Lambda}_k}{}^{H} \Phi_{\hat{\Lambda}_k})^{-1} \Phi_{\hat{\Lambda}_k}{}^{H}$.

Update the residual: $R_k = V - \Phi_{\hat{\Lambda}_k} \hat{\Theta}_k$.

if $\|R_k\|_2 \leq \varepsilon_1 \,||\, \left(\|R_k\|_2 / \left\| \Phi_{\hat{\Lambda}_k} \hat{\Theta}_k \right\|_2 \leq \varepsilon_2 \right)$

break;

end

$k = k + 1$;

End

Output: joint support set of the signal $\hat{\Lambda}_K$.

4 Simulation Results and Discussion

In our simulation, the correct support recovery of MWC refers to the criteria of the successful recovery in [8, 13], i.e., when the estimated support set $\hat{\Lambda}$ and real support set Λ meets the condition $\hat{\Lambda} \supseteq \Lambda$ and $\Phi_{\downarrow\hat{\Lambda}}$ is a full-rank matrix with columns. In order to validate the effectiveness of the proposed algorithm, signals with Sinc waveforms are

used to carry out simulations, and we compare the performances of SOMP and SwSOMP algorithms on the support recovery under different number of bands, sampling channel numbers, and SNRs.

The sparse wideband analog signal with noise is generated by

$$x(t) = \sum_{i=1}^{N/2} \sqrt{E_i B_i} \mathrm{sinc}(B_i(t-\tau_i)) \cos(2\pi f_i(t-\tau_i)) + n(t) \tag{9}$$

In (9), E_i, B_i, f_i and τ_i represent energy factor, bandwidth, carrier frequency and time offset of the produced ith signal, respectively. N represents the number of the symmetric bands. $n(t)$ is Gaussian white noise. The following procedure is repeated 500 times to calculate the percentage of correct support recovery.

(1) Generate the mixing signal $p_i(t)$ randomly;
(2) Generate the carrier frequency f_i in the interval $[-f_{nyq}/2, f_{nyq}/2]$ randomly;
(3) Generate new Sinc signal according to f_i;
(4) Using SOMP and SwSOMP respectively to estimate the support set and determine whether it is correctly recovered.

4.1 Impact of the Weakness Parameters on the Support Recovery

In the simulations, the parameters of the signal are $N = 6$ (3 pairs of symmetry), $E_i \in \{1, 2, 3\}$, $B_i \in \{50, 50, 50\}$ MHz, $\tau_i \in \{0.4, 0.7, 0.2\}$ μs, and carrier frequency f_i is randomly distributed in $[-f_{nyq}/2, f_{nyq}/2]$, and $f_{nyq} = 10$ GHz. The MWC sampling parameters are $L_0 = 97$, $L = 2L_0 + 1 = 195$, $f_s = f_p = f_{nyq}/L = 51.28$ MHz, and $m = \{15, 20, 25, 30, 35\}$. The reconstruction parameter is $\alpha \in (0, 1]$, and its initial value is 0.1 with 0.1 as the increasing interval, and here $Iters = 10$ because the iteration times of SWOMP has nothing to do with the signal sparsity. The $SNR = \{10, 20, 30\}$ dB. N is the band number of the signal, and m is the number of the MWC channels.

When α varies from 0.1 to 1, the percentage of correct support recovery is shown in Fig. 7 under the different number of channels m and different SNR. It can be seen from Fig. 7, SwSOMP algorithm performs best for the support recovery when $\alpha = 0.9$ for the effective channel number. Therefore, α is set to 0.9 in the following experiments.

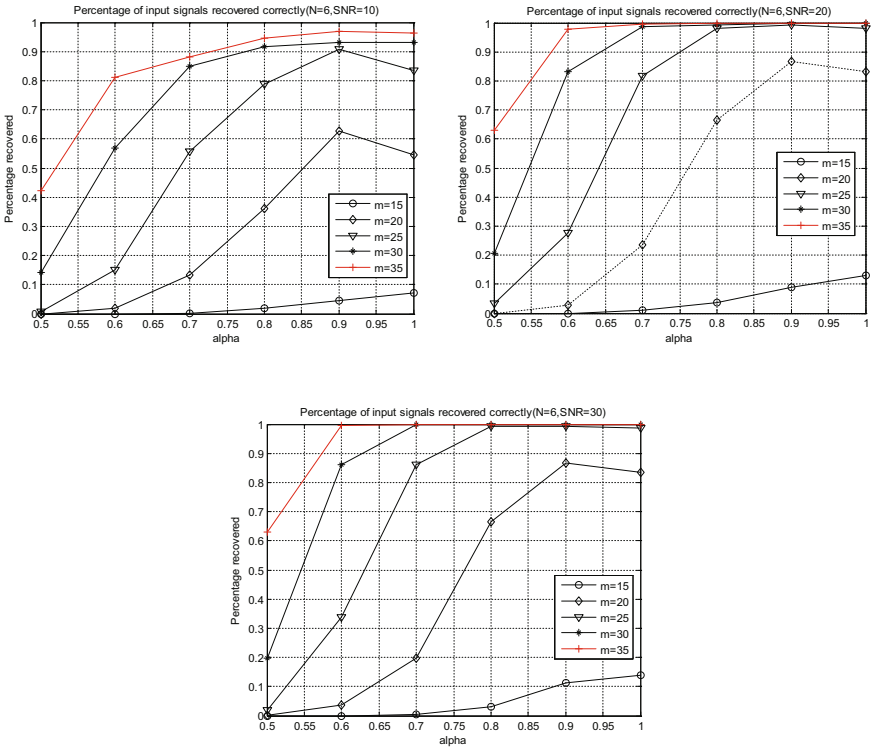

Fig. 7. Impact of α on the support recovery.

4.2 Impact of the Number of Sampling Channels on Support Recovery

The impact of the number of channels on the support recovery are investigated by using SOMP and SwSOMP algorithm. Figure 8 shows the percentages of correct recovery with SwSOMP and SOMP algorithms when the number of channels m is increased in the interval $[15, 40]$, and other parameters are the same as in Sect. 4.1. It can be seen from Fig. 8 that the performance of the recovery is improved by 12.4% when $m = 22$ with SwSOMP algorithm compared to that with SOMP algorithm. When $m = 25$, the percentage of correct recovery reaches 90% using SwSOMP algorithm, while the percentage of correct recovery can reach 90% when $m = 30$ using SOMP algorithm. Therefore, the SwSOMP algorithm can achieve higher reconstruction rate with less number of channels, which can save the hardware cost. Since the number of channels is directly related with the total sampling rate f_Σ ($f_\Sigma = mf_s$), SwSOMP algorithm can also reduce the system sampling rate by using less number of channels.

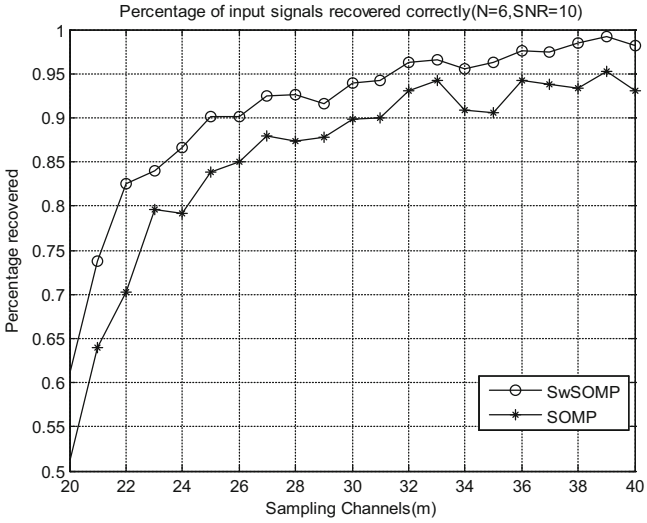

Fig. 8. Impact of the number of sampling channels on support recovery.

4.3 Impact of SNR on the Support Recovery

Now we consider about the impact of SNR on the support recovery by using two algorithms. The values of SNR are taken from the interval $[6, 20]$, $m = \{20, 25\}$, other parameters are the same as in Sect. 4.1. It can be seen from Fig. 9, when the number of channels is 25, SwSOMP algorithm achieves better recovery than SOMP algorithm in low SNR. When SNR = 6 dB and $m = 25$, the correct reconstruction with SwSOMP algorithm is improved 15% compared to that with SOMP algorithm. It can be seen that the correct reconstruction rate with SwSOMP algorithms is better than SOMP algorithm when the number of the channels is 20 and 25.

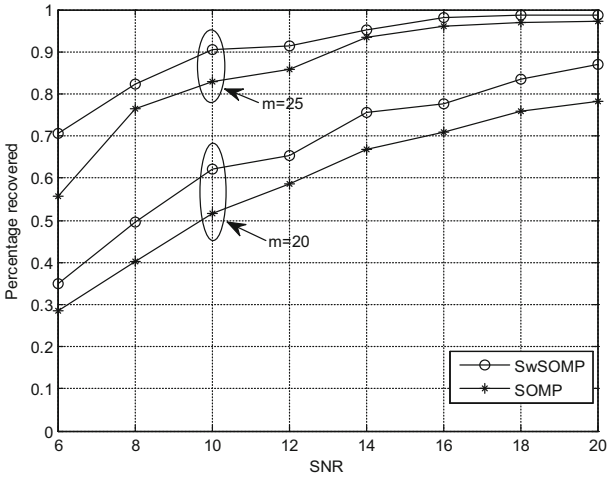

Fig. 9. Impact of SNR on the support recovery.

4.4 The Relationship Between the Number of Bands and the Support Recovery

The effects of number of frequency bands (i.e. signal sparsity) on the support recovery are investigated by using the two algorithms. The number of symmetric bands are taken from the interval $[2, 16]$. The relevant parameters setting are as follows, $SNR = 15$, $m = \{20, 25\}$, $E_i \in \{1, 2, 3, 4, 5, 6, 7, 8\}$, $\tau_i \in \{0.4, 0.7, 0.2, 0.9, 1.2, 1.5, 1.8, 2.1\}$ μs, and settings of other parameters are the same as in Sect. 4.1. It can be seen from the Fig. 10, when $N < 8$, the SwSOMP algorithm has a better performance. However, when $N = 8$, the performance has a sharp decline. It almost loses the ability of recovery when $N \geq 10$. It is mainly due to the fact that the signal can no longer be viewed as sparse signal under such circumstances. As a whole, SwSOMP algorithm performs better than SOMP algorithm under the cases of different number of bands.

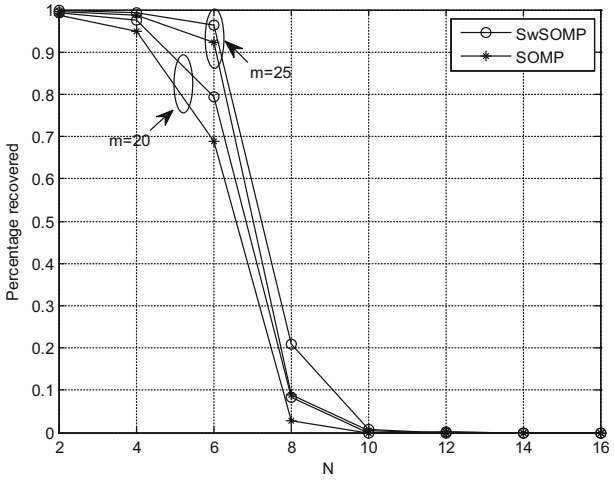

Fig. 10. The effects of number of signal bands on the support recovery.

5 Conclusion

Aiming to improve the performance of sensing multiband sparse signal in practice, this paper applies the SwSOMP algorithm to the CTF reconstruction block of MWC. The SwSOMP algorithm first obtains the largest matched inner-product value with the residual, which multiplies with the weakness parameter, and then obtains the atomic selection threshold. One or more atoms may be selected in each iteration, as a result of which the accuracy of matching the most relevant atoms is improved. Furthermore, the algorithm can reconstruct the support set of the signal blindly without knowing the signal sparsity in advance. By simulation experiments, we investigated the performance of SwSOMP algorithm in MWC and the impacting parameters. Compared with SOMP algorithm, SwSOMP algorithm has shown its advantages to be used in MWC for

spectrum sensing on improving the percentage of correct recovery, reducing the number of required sampling channels, and decreasing the total sampling rate of the system.

Acknowledgments. This paper was supported by the National Natural Science Foundation of China (Grant No. 61561017), Open Sub-project of State Key Laboratory of Marine Resource Utilization in South China Sea (Grant No. 2016013B), Hainan Province Natural Science Foundation of China (Grant No. 617033), Doctoral Candidate Excellent Dissertation Cultivating Project of Hainan University, and Postgraduate Practice and Innovation Project of Hainan University. Oriented Project of State Key Laboratory of Marine Resource Utilization in South China Sea (Grant No. DX2017012).

References

1. Cohen, D., Akiva, A., Avraham, B., et al.: Centralized cooperative spectrum sensing from sub-nyquist samples for cognitive radios. In: IEEE International Conference on Communications (ICC), pp. 8–12. IEEE Press, London (2015)
2. Walden, R.H.: Analog-to-digital converters and associated IC technologies. In: Proceedings of IEEE Compound Semiconductor Integrated Circuits Symposium, pp. 1–2. IEEE Press, Monterey (2008)
3. Candes, E.J., Wakin, M.B.: An introduction to compressive sampling. IEEE Signal Process. Mag. **25**(2), 21–30 (2008)
4. Healy, D., Brady, D.J.: Compression at the physical interface. IEEE Signal Process. Mag. **25** (2), 67–71 (2008)
5. Tropp, J.A., Laska, J.N., Duarte, M.F., et al.: Beyond Nyquist: efficient sampling of sparse band-limited signals. IEEE Trans. Inf. Theory **56**(1), 520–544 (2010)
6. Harms, A., Bajwa, W.U., Calderbank, R.: A constrained random demodulator for sub-Nyquist sampling. IEEE Trans. Signal Process. **61**(3), 707–723 (2013)
7. Zhao, Y., Wang, H., Zhuang, X., et al.: Frequency domain sensing system using random modulation pre-integrator. IET Sci. Meas. Technol. **7**(3), 166–170 (2013)
8. Mishali, M., Eldar, Y.C.: From theory to practice: sub-Nyquist sampling of sparse wideband analog signals. IEEE J. Sel. Top. Sign. Process. **4**(2), 375–391 (2010)
9. Eldar, Y.C., Levi, R., Cohen, A.: Clutter removal in Sub-Nyquist radar. IEEE Signal Process. Lett. **22**(2), 177–181 (2015)
10. Lexa, M.A., Davies, M.E., Thompson, J.S.: Reconciling compressive sampling systems for spectrally sparse continuous-time signals. IEEE Trans. Signal Process. **60**(1), 155–171 (2012)
11. Shilian, Z., Xiaoniu, Y.: Wideband spectrum sensing in modulated wideband converter based cognitive radio system. In: 11th International Symposium on Communications and Information Technologies, pp. 114–119. IEEE Press, Hangzhou (2011)
12. Cohen, D., Akiva, A., Avraham, B., et al.: Distributed cooperative spectrum sensing from Sub-Nyquist samples for cognitive radios. In: 16th International Workshop on Signal Processing Advances in Wireless Communications (SPAWC), pp. 336–340. IEEE Press, Stockholm (2015)
13. Mishali, M., Eldar, Y.C.: Blind multiband signal reconstruction: compressed sensing for analog signals. IEEE Trans. Signal Process. **57**(3), 993–1009 (2009)
14. Tropp, J.A., Gilbert, A.C., Strauss, M.J.: Algorithms for simultaneous sparse approximation. Part I: greedy pursuit. Signal Process. **86**(3), 572–588 (2006)

15. Chen, J., Huo, X.: Theoretical results on sparse representations of multiple-measurement vectors. IEEE Trans. Signal Process. **54**(12), 4634–4643 (2006)
16. Blumensath, T., Davies, M.E.: Stagewise weak gradient pursuits. IEEE Trans. Signal Process. **57**(11), 4333–4346 (2009)
17. Donoho, D.L., Tsaig, Y., Drori, I., et al.: Sparse solution of underdetermined systems of linear equations by stagewise orthogonal matching pursuit. IEEE Trans. Inf. Theory **58**(2), 1094–1121 (2012)
18. Yang, P., Fan, Y., Huang, Z.T., et al.: Single channel spectrum sensing technique based on sub-Nyquist sampling. J. Natl. Univ. Defense Technol. **35**(4), 121–127 (2013)
19. Landau, H.J.: Necessary density conditions for sampling and interpolation of certain entire functions. Acta Math. **117**, 37–52 (1967)